

Fermi National Accelerator Laboratory

FERMILAB-Conf-92/333

**Particle Tracking in $E - \phi$ Space for
Synchrotron Design and Diagnosis**

J.A. MacLachlan

*Fermi National Accelerator Laboratory
P.O. Box 500, Batavia, Illinois 60510*

November 1992

Presented at the *12th International Conference on the Application of Accelerators in Research and Industry*,
Denton, Texas, November 2-5, 1992

Disclaimer

This report was prepared as an account of work sponsored by an agency of the United States Government. Neither the United States Government nor any agency thereof, nor any of their employees, makes any warranty, express or implied, or assumes any legal liability or responsibility for the accuracy, completeness, or usefulness of any information, apparatus, product, or process disclosed, or represents that its use would not infringe privately owned rights. Reference herein to any specific commercial product, process, or service by trade name, trademark, manufacturer, or otherwise, does not necessarily constitute or imply its endorsement, recommendation, or favoring by the United States Government or any agency thereof. The views and opinions of authors expressed herein do not necessarily state or reflect those of the United States Government or any agency thereof.

Particle Tracking in $E - \phi$ Space for Synchrotron Design and Diagnosis*

J. A. MacLachlan

Fermi National Accelerator Laboratory, Batavia IL 60510[†]

4 November 1992

Abstract

The single particle equations for the longitudinal motion in a synchrotron can be faithfully represented as a one-turn mapping of a particle's phase space position relative to the synchronous particle. Applied to a distribution of particles, the mapping can be used to model the evolution of bunches to test beam manipulations or to extract the time dependence of quantities like the bunching factor, momentum spread, *etc.* which can be difficult to calculate. Such modelling requires rather few representative particles, permitting numerical experimentation and exploratory design trials. By modifying the mapping each turn to introduce the collective effects of the distribution, one can model such processes as phase feedback, space-charge effects, coupled bunch motion, *etc.* Calculations of this type offer quantitative performance predictions, aid diagnosis of existing accelerators, and contribute to the understanding of the underlying dynamics. This talk introduces the tools and some illustrations.

Introduction

The technique of turn-by-turn tracking of the transverse motion of representative beam particles is commonly used to determine dynamic aperture, resonance widths, sensitivity to field and alignment errors, *etc.* for circular accelerators. Longitudinal motion is generally ignored or considered only as the cause of a periodic modulation of the momentum spread or momentum error. In proton synchrotrons transverse focusing produced by the quadrupole magnetic field may be 10^8 times the longitudinal focusing arising from the slope of the rf waveform so that the frequency of transverse oscillation may be $\sim 10^1$ /turn while the longitudinal oscillation frequency is $\sim 10^{-3}$ /turn. In such a circumstance the transverse and longitudinal degrees of freedom are practically decoupled and are almost always treated independently. Far more effort has been devoted to understanding the problems related to transverse motion,

*Presented at 12th International Conference on the Application of Accelerators in Research and Industry, Denton TX, 2 - 5 November 1992

[†]Work supported by the U. S. Department of Energy contract No. DE-AC02-76CHO3000.

and there are now several widely used codes for tracking. Nonetheless, there are processes like rf capture and transition crossing depending essentially on longitudinal dynamics which can be very important in determining accelerator efficiency. Furthermore, intricate rf manipulations to optimize longitudinal phase space properties of the beam for special applications have been becoming increasingly common, especially with the development of hadron colliders.

Preparation of high brightness bunches for the Tevatron collider depends on rf gymnastics both to maximize the \bar{p} production and to prepare bunches for collision.[1],[2] Simulation of these manipulations by tracking appropriate distributions has been used to find optimum parameters. Usually single particle dynamics are appropriate for modelling the motion and often all nonlinearity except that of the rf potential can be ignored. In this case the calculations go quickly, and detailed optimization is possible by making many trials.

Often, however, the collective effect of the distribution on the particle motion through feedback loops, wakefields, beam loading, *etc.* plays an essential role in the process to be modeled. Then the map for each particle must be modified to reflect its energy increment from the collectively produced field. When this is so, the computing load may prohibit a large number of trials. However, if beam and system parameters can be chosen realistically, one can get an excellent indication of what to expect from a real accelerator. Such multi-particle simulations may be even more useful after a machine is built as one attempts to understand beam behavior by establishing a model of sufficient validity and completeness to reproduce the observations. A model in good accord with the known system parameters and beam observations is a powerful tool in developing a more complete and fundamental knowledge of the beam and its environment. The results of the simulation of particular systems can also be a useful guide in working out an analytical treatment of the phenomena.

There are a few computer programs for longitudinal phase space tracking available to interested users; see for example refs. [3],[4], and [5]. For the ESME code there has been at least some use at several laboratories and some features have been introduced in response to the interests of a small community of users. The following introduction to the fundamentals and some applications is grounded in the author's development of ESME but is intended to be general enough to be helpful to someone who will use another code or write a new one. A number of references are cited which give additional details in a form consistent with that of this presentation; no attempt has been made here to identify original sources.

Fundamentals

The single particle equations for the longitudinal motion in a synchrotron are naturally formulated as a pair of first order nonlinear difference equations directly from consideration of the physical system.[6] One equation gives the phase slip between a particle and a synchronous reference particle during the passage between rf gaps, and one gives the energy change at the gap:¹

¹The derivation given in the reference is elementary but reasonably complete. Not included are terms important only when rf parameters change very quickly, *i.e.*, by a significant amount per turn. The absence of an explicit betatron acceleration term is better explained in ref. [7].

$$\begin{aligned}
\varphi_{i,n} &= \frac{\omega_{s,n}}{\omega_{s,n-1}}\varphi_{i,n-1} + 2\pi h(S_{i,n} - 1) \\
W_{i,n} &= \frac{\omega_{s,n-1}}{\omega_{s,n}}W_{i,n-1} + \frac{e}{\omega_{s,n}}[V(\varphi_{i,n} + \phi_{s,n}) - V(\phi_{s,n})] .
\end{aligned} \tag{1}$$

The quantities appearing in eqs. 1 are understood as follows:

i refers to a particle of interest.

s refers to the synchronous particle.

n refers to the n -th turn ended by the n -th energy kick.

h is the integer ratio of rf frequency to synchronous circulation frequency.

$$\omega = h\Omega = hv/R$$

ϕ is particle phase, *i.e.*, rf phase when particle is at gap.

$$\varphi_{i,n} = \phi_{i,n} - \phi_{s,n}$$

$W_{i,n} = (E_{i,n} - E_{s,n})/\omega_{s,n}$, where the E 's are total energy.

$S_{i,n} = \omega_{s,n}/\omega_{i,n}$ is the phase slip per turn.

These equations provide a map of the W, φ phase space onto itself. The Jacobian is identically one, so the map is area conserving to all orders. Someone working with an analytical approach might regard them as a symplectic integration scheme for the Hamilton's equations derived from a continuous Hamiltonian for the problem. However, essentially no approximation is required to derive the difference equations beyond the two rather physical assumptions already mentioned, *viz.*, impulsive energy increment and no significant change in parameters between steps. Note in this context that the iteration step need not be a full turn around a synchrotron; if some extreme case requires, the parameters can be updated several times per turn with partial turn maps. Therefore, one might equally well regard the differential equations and their associated Hamiltonian as providing a continuous approximation to an essentially discrete process. Certainly if the object is computer modeling, one has nothing to gain by numerical solution of Hamilton's equations; the full dynamical possibilities are inherent in the difference equations in a form that is practically an algorithmic statement as it stands.

For convenience in modeling it will be useful to rewrite the difference equations in coordinates $\varepsilon_i = E_i - E_s$ and $-\pi \leq \vartheta_i = \varphi_i/h \leq \pi$, where E_i is the total energy of particle i and ϑ_i is effectively² the particle azimuth in the ring when the synchronous particle is at the gap ($\vartheta = 0$) except that the particles circulate in the $-\vartheta$ direction. This angular variable is not entirely conventional, but it has some convenience.

$$\begin{aligned}
\vartheta_{i,n} &= \frac{\omega_{s,n}}{\omega_{s,n-1}}\vartheta_{i,n-1} + 2\pi(S_{i,n} - 1) \\
\varepsilon_{i,n} &= \varepsilon_{i,n-1} + eV(\vartheta_{i,n}) - eV(0) .
\end{aligned} \tag{2}$$

²“Effectively” but not precisely; see ref. [6], pp 6-7.

The language used here corresponds to a model in which there is one energy kick per turn. The proper generalization for those few cases where there is need for partial turn maps is to reduce the range of ϑ correspondingly. These new variables are not canonically conjugate. However, the rms area of the distribution can be easily converted to units of eVs; this quantity is then conserved for a matched distribution.

Either of the equations 1 or 2 are quite general. No assumption that $E_i - E_s \ll E_s$ has been made nor is there any assumption about $V(\vartheta)$ other than $[V(\vartheta+2\pi) - V(\vartheta)]/V(\vartheta) \ll 1$ for all ϑ , i.e., that $V(\vartheta)$ is nearly periodic with at least period 1; if it has higher periodicity, the potential is said to have harmonic number $h > 1$. If the initial distribution as well as the potential has higher periodicity one can exploit the periodicity in the calculation and consider only one period of the azimuthal distribution. Even so, it is a good idea to retain the ϑ variable with a range of 2π for the whole azimuth; in any case where rf systems with different harmonic numbers are used it simplifies the definitions of relative phases and the synchronous phase for the composite potential.

The difference equations eqs. 2 contain essentially all of the dynamical possibilities of the longitudinal motion, but in most applications the effects of the momentum dependence of velocity or path length above first order are negligible. Generally the higher order terms will have a distinctive role only near transition energy, where the first order term in the phase slip equation vanishes, or at a very low energy, where velocity is a strong function of energy. Eqs. 2 represent slightly different maps for each individual particle. By dropping terms above first order one can write a map which is the same for all particles; the only remaining nonlinearity is that of the rf potential, which is the fundamental concern in most simulations. The map

$$\begin{aligned}\vartheta_{i,n} &= \vartheta_{i,n-1} + \frac{2\pi\eta}{\beta_s^2 E_s} \varepsilon_{i,n-1} \\ \varepsilon_{i,n} &= \varepsilon_{i,n-1} + eV(\vartheta_{i,n}) - eV(0)\end{aligned}\tag{3}$$

is far simpler than eq. 2 and need be calculated only once per turn. The quantity η is the time dispersion $\gamma_t^{-2} - \gamma_s^{-2}$. Using this map brings some interesting problems into the reach of hand calculator computation. When computer time is a consideration, it can be useful to employ this map during the checkout phase even in cases where some effect is expected from the higher order terms; when all the mechanics have been worked out one can substitute the more complete map for final runs. Besides cases at low energy or energy near transition the full map may be important in applications like rf stacking or displacement acceleration where the difference between particle energy and synchronous energy can be unusually large, making higher order terms significant even though the coefficients are small.

RF Waveform

The functional form of the rf waveform has not been specified. It is very likely to be a sinusoid of course. By providing for a sum of sinusoids one automatically satisfies the periodicity and provides for multiple conventional rf systems or the fourier series representation of an arbitrary waveform. When something more complicated than a single sinusoid is employed,

the definition or determination of the synchronous phase may not be obvious. This complication has been dealt with in ESME by defining all rf phases ψ_{jn} relative to $\vartheta = 0$ at time t_{sn} . Thus,

$$V_n(0) = \sum_{k=1} v_{kn} \sin(k\theta_{sn} + \psi_{kn}) \quad (4)$$

and

$$V_n(\vartheta_{in}) = \sum_{k=1} v_{kn} \sin[k(\vartheta_{in} + \theta_{sn}) + \psi_{kn}] \quad (5)$$

so that θ_{sn} is the amount by which the arbitrary waveform must be shifted to make $\vartheta_{sn} \equiv 0$. If the tracking code is to shift the rf phase to maintain synchronism between prescribed momentum and rf voltage programs, θ_{sn} is calculated by numerical solution of

$$\dot{p}_{sn} = eV(\theta_{sn})/C_{sn} \quad V'_n(\theta_{sn}) \times (E_T - E_{sn}) > 0 \quad , \quad (6)$$

where C_{sn} is the length of the synchronous trajectory and where the second condition selects the stable fixed point according to whether the synchronous energy E_{sn} is below or above the transition energy E_T . This solution gives the amount by which the waveform must be translated to keep a bunch centered at $\vartheta = 0$ synchronized. This choice of independent quantities is typical, but one may just as well choose to have the voltage controlled to follow a prescribed phase program, or prescribe both voltage and phase, taking the synchronous radius as a result. It is certainly possible to take rf frequency as an independent quantity, but this is usually not convenient; the frequency is more often taken as a result. It is unlikely that an *a priori* frequency program will preserve a constant synchronous orbit without radial feedback.³

Feedback and Almost Independent Particle Motion

The introduction of feedback to phase, frequency, or voltage based on bunch centroid, radial position, or shape oscillation respectively takes the calculation in principle from single particle dynamics to collective motion. However, because only first or second moments of the distribution enter and they act by altering the map in the same way for all particles, very little additional calculation is required. Effects such as space charge or the various manifestations of wakefields which depend on details of the distribution like its fourier spectrum and act differentially on the distribution require many more macroparticles to represent the beam adequately and more elaborate analysis to extract the relevant beam properties. Collective motion of the first sort is easily included in small-scale calculations; the second type of problem introduces considerable additional complexity which will be addressed in a later section.

Fast feedback from mean bunch phase to the phase of the rf drive is the most fundamental low-level feedback loop. The simplified map makes a good point of departure for understanding how it works and how it is implemented. Going from the finite difference

³Radial feedback is not implemented in ESME, but the radial error history can be used *a posteriori* to improve a prescribed frequency program.

equations eqs. 3 to the corresponding pair of differential equations and using just a linear approximation for the rf waveform, one may write

$$\begin{aligned}\frac{d\varphi}{dn} &= \frac{2\pi h\eta}{\beta^2 E_s} \varepsilon \\ \frac{d\varepsilon}{dn} &= e\mathbf{V} \cos \phi_s .\end{aligned}\quad (7)$$

Combining the first order equations one arrives at a second order equation for the phase for small oscillations

$$\varphi'' + \nu_s^2 \varphi = 0 , \quad (8)$$

where ν_s is the synchrotron tune

$$\nu_s = \sqrt{\frac{-2\pi h\eta \mathbf{V} \cos \phi_s}{\beta^2 E_s}} . \quad (9)$$

This is a linear equation, so not only does it apply to each particle individually but also to the motion of the bunch centroid $\bar{\varphi}$, so long as all of the amplitudes are small. Adding to this equation a term proportional to $-\bar{\varphi}'$ will lead to a damping of the oscillation:

$$\bar{\varphi}'' + \nu_s^2 (g\bar{\varphi}' + \bar{\varphi}) = \bar{\varphi}'' - 2\alpha\bar{\varphi}' + \nu_s^2 \bar{\varphi} = 0 , \quad (10)$$

where g is the feedback gain and $d\bar{\varphi}/dn$ will be determined by differencing the measured centroid phase turn-by-turn. The solution of eq. 8 may be written as

$$\bar{\varphi}(n) = \bar{\varphi}_0 e^{-\alpha n} \cos \beta n , \quad (11)$$

where

$$\beta^2 = \nu_s^2 - \alpha^2 . \quad (12)$$

The fastest damping occurs for $\beta = 0$ (critical damping) for which the gain is to be

$$g_c = -\frac{2}{\nu_s} . \quad (13)$$

Although the eqs. 2 describe a nonlinear dynamical system, subtracting $2(\bar{\varphi}_n - \bar{\varphi}_{n-1})/\nu_s$ from the phases $\varphi_{i,n}$ each turn will damp the motion of the bunch centroid. A simulation of phase feedback can be made more realistic by evaluating $d\bar{\varphi}/dn$ as a weighted average over several turns, the weights giving the high frequency behavior of the transfer function of the loop and the number of turns averaged giving the lower cutoff.[8] For any case other than small oscillations and infinite bandwidth feedback, one may expect that the optimum gain is not exactly g_c .

Application to Bunch Coalescing

Even in a conventional synchrotron acceleration cycle, there are processes which, though understood in principle, are not amenable to quantitative calculation by analytical techniques. Examples include rf capture, transition crossing, and response to errors or noise in the rf. For these problems the single particle map plus, perhaps, feedback to the rf parameters can be used to get detailed results for a specific set of conditions so long as the effects of the beam current and space charge are not the important considerations. The process of combining several consecutive bunches into a single bunch at the same rf harmonic number will be used to illustrate several ideas in a single example. This is not exactly a standard operation, but such bunch coalescing is illustrative of the kind of rf gymnastics which are a routine part of preparing high intensity bunches for the Tevatron collider.[2]

Initial Distribution

For this particular example the exact manner in which the macroparticles are distributed to represent the initial bunches is not a major consideration. However, in some cases a realistic answer depends critically on starting from a realistic initial phase space distribution; usually that will mean a distribution matched to the initial Hamiltonian. A distribution function will be matched to the Hamiltonian if it is a function of it. The elliptical distribution[9] is a function of the Hamiltonian which is typical of proton bunches. It can be constructed for an arbitrary rf waveform by using the difference equations to trace the bunch boundary which is then filled by selecting random ϑ values and choosing a companion ϵ from an elliptic distribution bounded by the upper and lower energy at that ϑ . The failure to use a matched distribution will result in fluctuation of the rms emittance. On the other hand, for illustrating the phase space structure of the particle motion it is often useful to distribute macroparticles on parallel lines or on closed contours. There is only one really general way to achieve a matched distribution, namely to start from one for a simple case like no rf voltage and to introduce the rf and any other perturbations slowly so that the particle flow can adjust. This is the process of adiabatic capture. For what follows it will be appropriate to represent each of the initial bunches by an elliptical distribution determined by the initial rf parameters.

The Coalescing Process

Coalescing is achieved by changing from the initial harmonic number to a lower one at an intermediate stage and then back to the original. If there is sufficient time available and bunch momentum spread does not fall below the microwave instability threshold, it is possible to carry out the changes so that the coalesced bunch area is practically the sum of the areas of the initial bunches. The steps in such a quasi-adiabatic coalescing are illustrated by the phase space plots in figs. 1 - 5. Fig. 1 shows nine consecutive bunches of 0.3 eVs nearly filling 53 MHz ($h=588$) buckets produced by 10 kV. The accelerator parameters are those of the Fermilab Main Injector given in the table.

Table: Main Injector Parameters

mean radius	538.302	m
γ_T	20.4	
energy for Tevatron injection	150.	GeV
rf harmonic number h	588	
maximum rf volts	4.0	MV
harmonic number for coalescing	28	
maximum rf volts for coalescing	22.5	kV
harmonic number for bucket shaping	56	
rf voltage for bucket shaping	~ 4	kV
typical longitudinal emittance (95%)	0.3	eVs
typical protons per bunch	3.3	$\times 10^{10}$
coupling impedance $Z_{ }/n$	5.0	Ω

The beam is debunched by lowering the 53 MHz voltage so that the adiabaticity parameter $\alpha = \frac{\gamma_{\text{synch}}}{S_B} \frac{dS_B}{dt}$ is constant at -0.45. The debunching is carried out with 250V of 2.5 MHz ($h=28$) and 125 V of 5.1 MHz ($h=56$) rf present. The effects of the low frequency systems are not apparent at the initial level of the 53 MHz system, but the 53 MHz voltage is slowly lowered so that the $h=588$ buckets eventually become full and then start to lose particles (fig. 2). The $h=28$ voltage is chosen so that at this point the effective bucket is a highly perturbed $h=28$ bucket; the particles lost from the disappearing $h=588$ buckets find themselves on closed $h=28$ phase space trajectories just outside the $h=588$ stable areas.[10] As the 53 MHz voltage is further reduced, the $h=28$ bucket takes on a more normal outline (fig. 3). However, the $h=56$ has been chosen to reduce the curvature of this bucket in the central portion which spans the original nine bunches, thereby providing a better match to the baton shape formed from the bunches of equal height. The next step is to raise the $h=28$ and $h=56$ voltages so that the coalesced distribution rotates in a mismatched bucket (fig. 4). In this step the $h=56$ amplitude is chosen to make the synchrotron frequency nearly independent of amplitude for the amplitudes spanned by the bunch. The final step shown in fig. 5 is to re-introduce the $h=588$ voltage at a high level to match the rotated bunch when it reaches minimum width. The emittance dilution following this step could be reduced significantly by adding $h=1176$ voltage to provide a bucket better matched to the rotated baton of charge, but no such rf system is planned for the Main Injector. Therefore, the effective emittance of the coalesced bunch will grow by filamentation to nearly the area of the capturing bucket. This example has not been chosen to demonstrate the minimum possible dilution. Antiproton coalescing, for example, does not have this complication of shape mismatch because the initial bunches, being produced by adiabatic capture from a single long bunch in the Accumulator, have a bunch height sequence which matches the shape of an ordinary bucket.

In one respect this is not such a good example of the application of single particle dynamics, because, with the beam current and longitudinal coupling impedance of the Main Ring, it is not possible to carry out the initial debunching to such low momentum spread. However, it was just this kind of idealized simulation that was used to demonstrate the concept and work out the basic parameters. In the next section the same process is considered with the inclusion of space charge and a broadband coupling impedance as an example of some techniques in multi-particle problems.

Collective Effects in Bunch Coalescing

Although the coalescing process described above did permit the preparation of bunches of $> 10^{11}$ protons for the Tevatron collider, it has never produced the beam brightness or lack of satellite bunches shown in the single particle simulations. The observation of a lower limit on the attainable momentum spread indicates that the process may be reaching an instability threshold. The possibility that the limitation arises from single-bunch coherent longitudinal instability (microwave instability) was illustrated by simulation,[11] but it appears that there are additional problems of beam loading and longer range coupling as well.[12],[13] These sources of coupling can also be included in a simulation,[14] but it will be a sufficient introduction to consider simply a broadband impedance.

Self Field and Longitudinal Impedance

Because only the longitudinal coordinates will be considered, the force on individual particles resulting from the beam current distribution must be modeled in some way that averages over transverse coordinates. Fortunately, as will appear in the following, its effect is usually small in proton synchrotrons so that a simple approximation is adequate. There are cases like injection in high intensity machines where more precise treatment may be useful. Here, following the approach of Neil and Sessler,[15] the beam is treated as a circular cylinder of charge with density independent of radius out to the fixed radius a of the cylinder but varying along the orbit. The beampipe is treated as a perfectly conducting cylinder of radius b . The electrostatic field is calculated in the beam rest frame and the result transformed to the lab frame to find the longitudinal Lorentz force on the beam particles.[16] By integrating the force over a turn one finds an accelerating or decelerating voltage proportional to the beam current. The proportionality between the beam current and this voltage is an imaginary, frequency dependant impedance:

$$\frac{Z_{sc}}{n} = -i \frac{Z_o g}{2\beta\gamma^2} , \quad (14)$$

where $Z_o = (\epsilon_o c)^{-1} = 377\Omega$, the geometric factor $g = 1 + 2\log(b/a)$, and β and γ are the Lorentz velocity and energy parameters. The impedance is capacitive in sign, but the frequency dependence is that of an inductance, being given by n^{-1} , where n is the harmonic number relative to the circulation frequency. The result applies to other beampipe geometry with an appropriate effective ratio b/a .

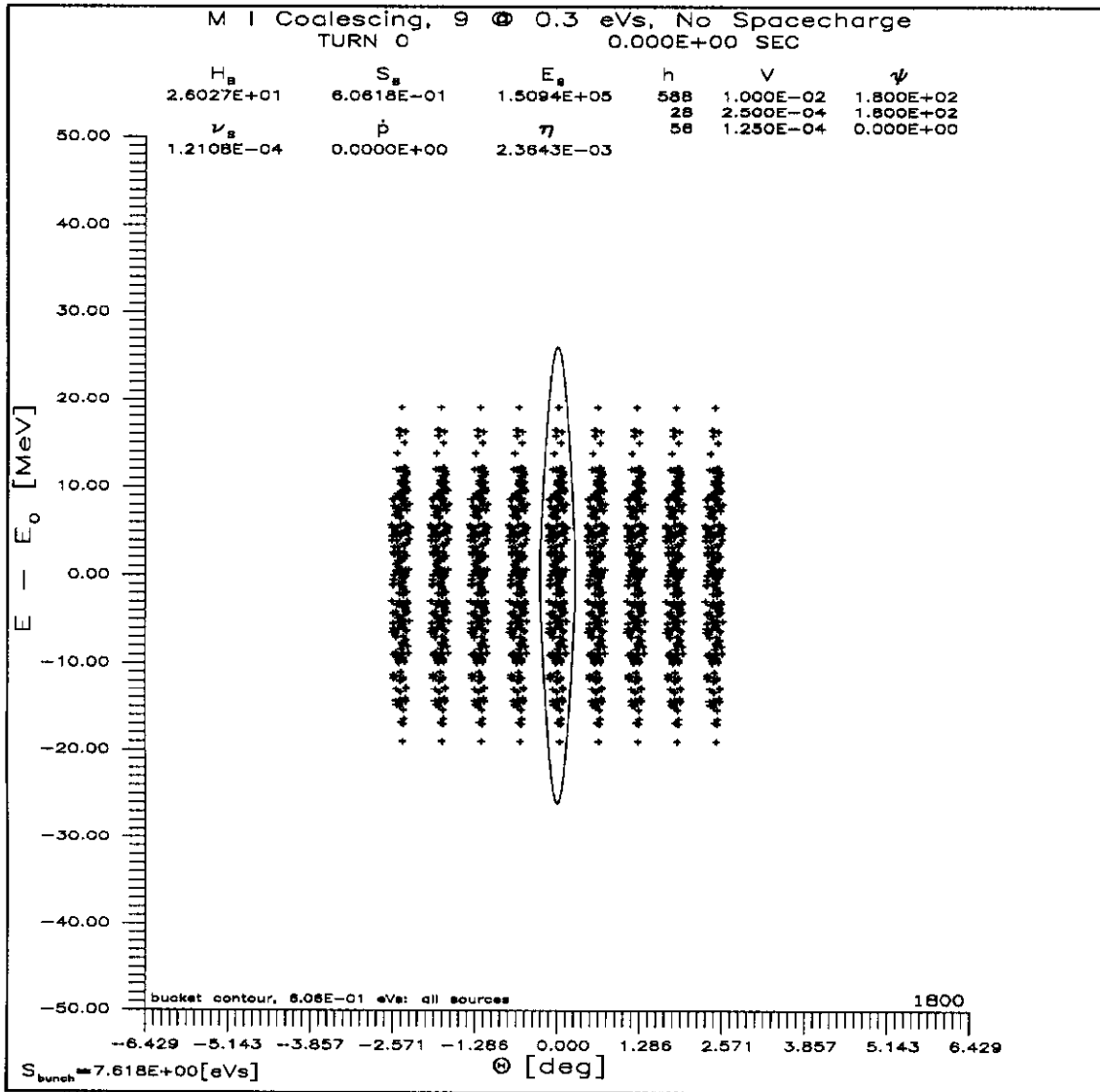


Figure 1: Nine 0.3 eVs Main Injector bunches matched to 10 kV of 53 MHz ($h=588$) rf on a 150 GeV flattop. The $h=28$ and $h=56$ coalescing systems are on.

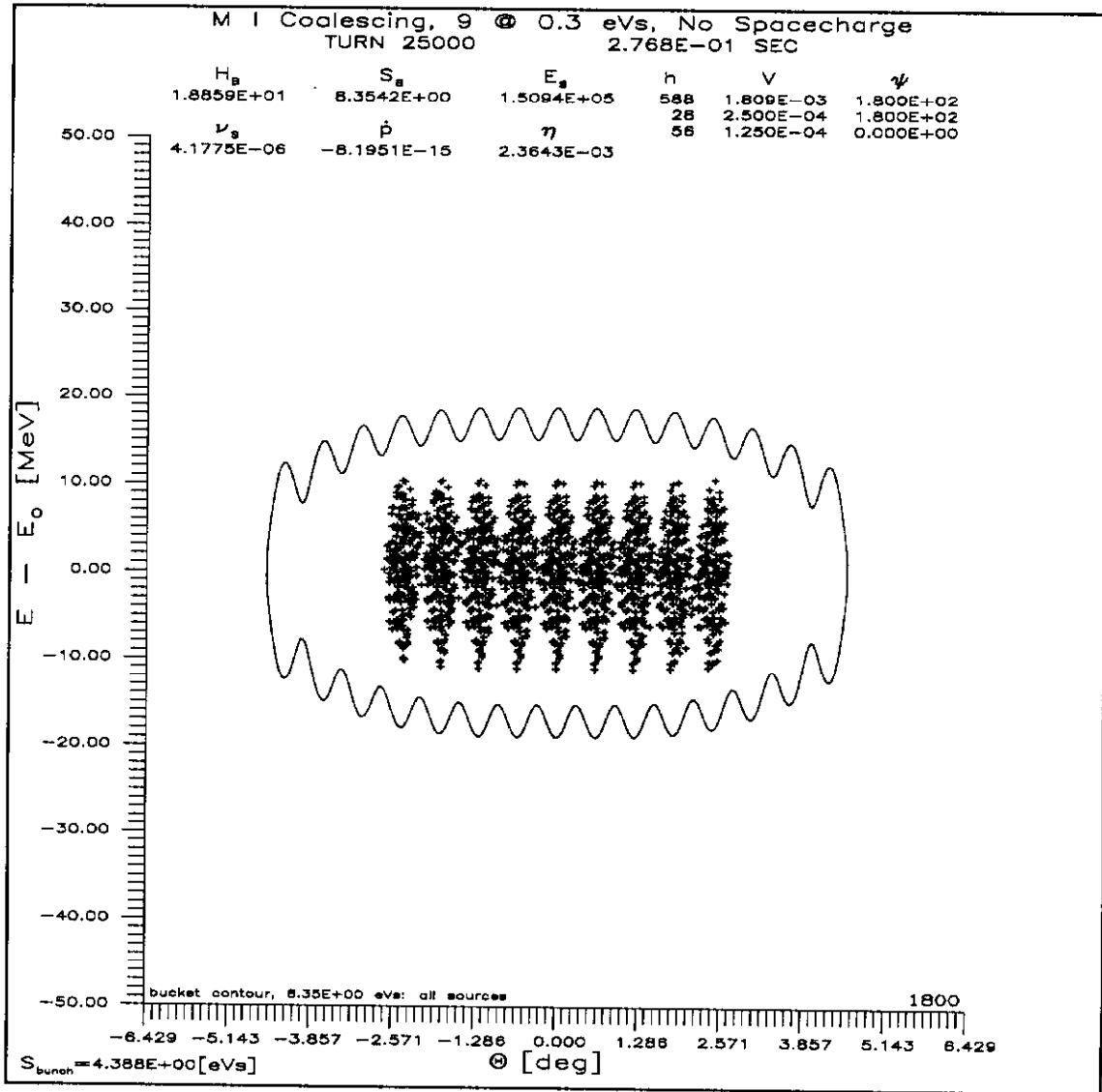


Figure 2: Debunching process after 0.28 s; the $h=1113$ buckets are just starting to lose protons.

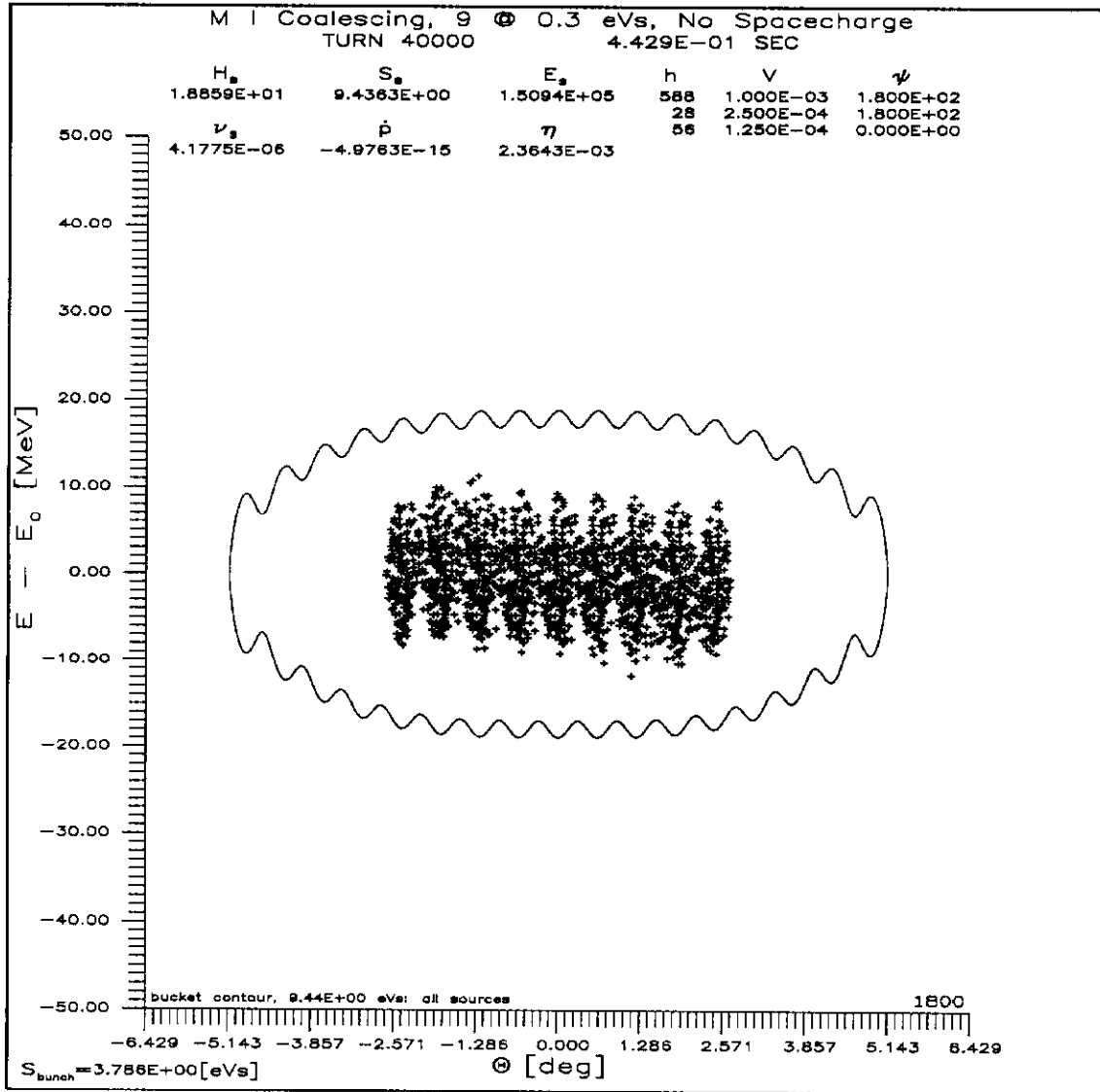


Figure 3: Debunching process after 0.43 s; the debunching is not complete, but the distribution is approaching that expected for the $h=28$ and $h=56$ systems alone.

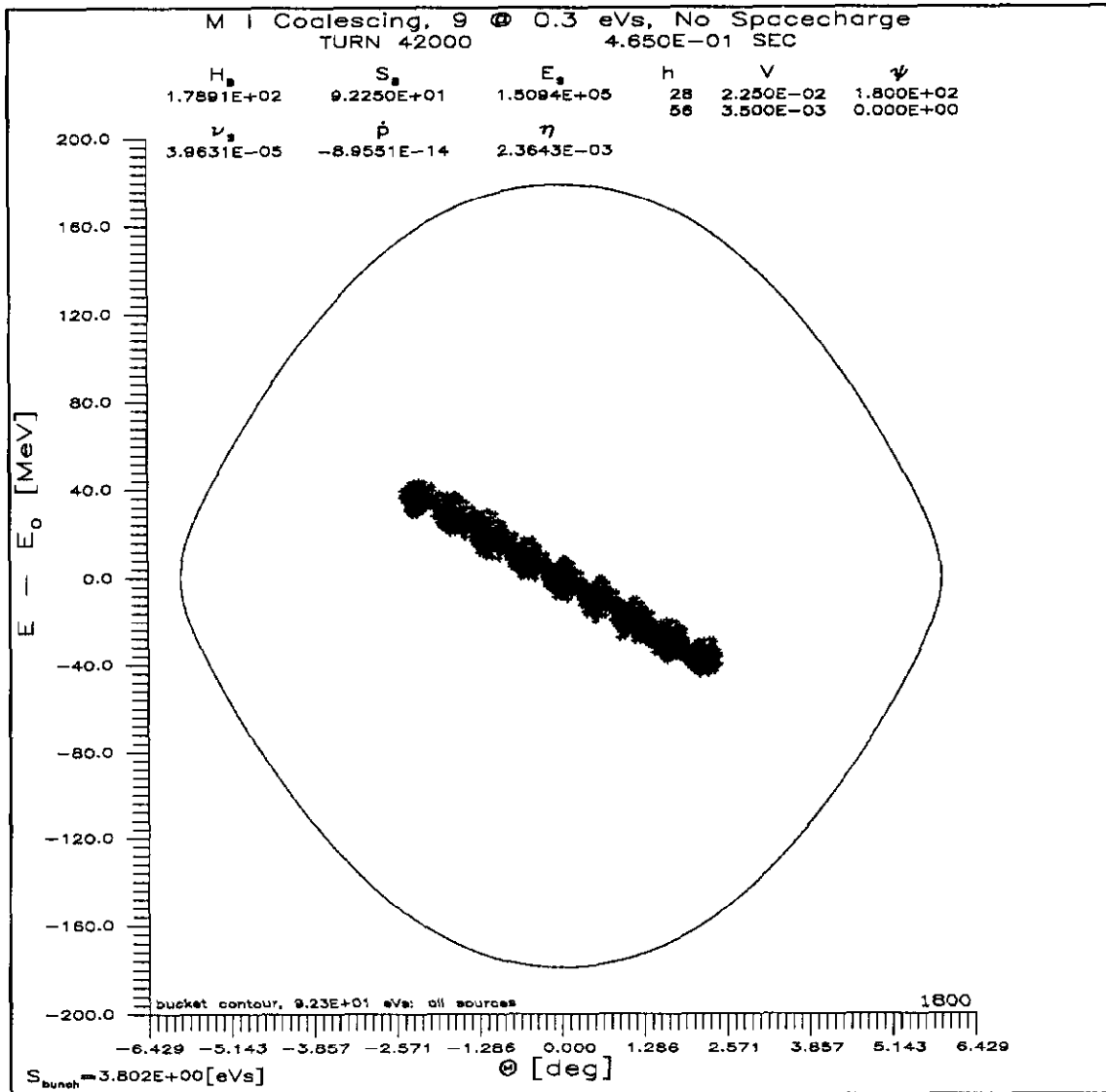


Figure 4: Rotation of distribution in h=28 bucket linearized by an h=56 component.

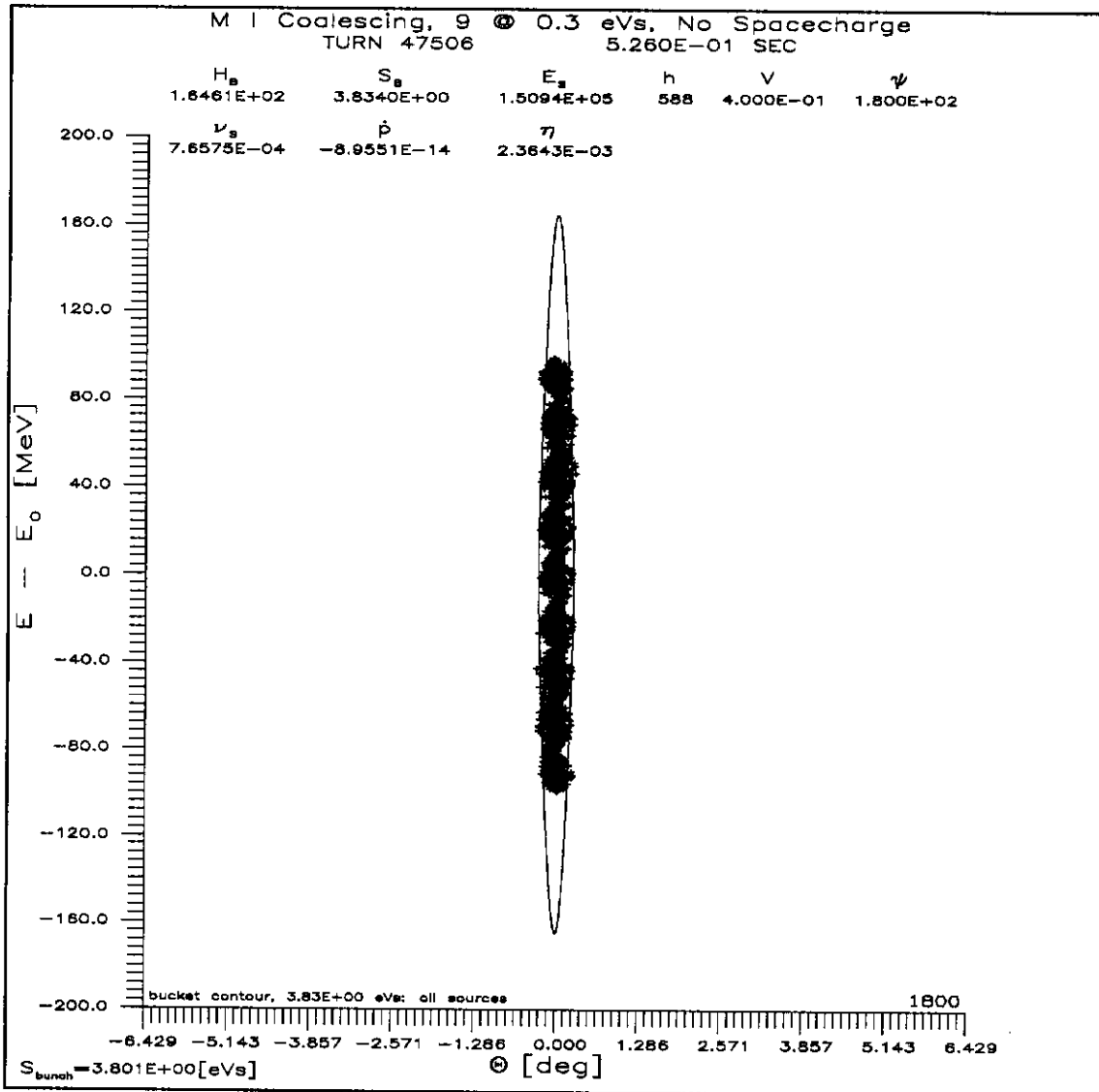


Figure 5: Recapture of rotated distribution at $h=1113$. This recapture is not 100 % efficient, and the shape mis-match will result eventually in dilution of the captured portion to nearly the area of the capturing bucket.

Having expressed the space-charge force via an impedance, one can easily combine it with the forces resulting from the interaction of the beam current with its surroundings. Consider the image of the beam current flowing in the beampipe. There is clearly a real surface resistance and an inductive term. This is the resistive wall term, which is most important at low multiples of the circulation frequency. There may as well be several resonant contributions resulting from rf cavities, special devices like kickers and beam monitors, and miscellaneous discontinuities in beampipe size. Many of these impedances can be calculated from first principles and most can be measured on the bench. In the end there is generally some broadband residue which can be measured with the beam but can not be definitively identified with particular sources. To proceed more or less realistically without the complication of the peculiarities of some particular accelerator, a broadband impedance will be used which is representative of the general frequency dependence of impedance in many machines, particularly in the high frequency region from the microwave cutoff of the beampipe down two or three octaves. The widely used model is a resonance at the microwave cutoff ω_{co} with $Q = 1$ and a real value of $Z_{||}/n$ at resonance of a few ohms:

$$Z_{||} = \frac{R_{sh}}{1 + i(n\Omega/\omega_{co} - \omega_{co}/n\Omega)} \quad (15)$$

The value of $Z_{||}/n$ at the resonant frequency ω_{co} is $R_{sh}/n\omega_{co}$. It is loosely speaking a measure of the smoothness of the beampipe and can be reduced to as little as one ohm by careful design. Because the Q is very low and the resonance is in the GHz range, this impedance represents the short range wakefield that couples primarily particles within the same rf bunch. The instability arising when this impedance exceeds a threshold

$$Z_{||}^{(th)}/n = \frac{F\beta^2 E \eta}{e\hat{I}} \left(\frac{\Delta p}{p} \right)_{FWHM}^2 \quad (16)$$

is called microwave instability. Basically it is self-bunching of the beam by the voltage resulting from the image current flowing in $Z_{||}$. The threshold can be determined up to a form factor of order one by calculating the impedance at which any Fourier component of the beam current can generate a bucket with height greater than the local $\Delta p/p$ of the distribution. By linearizing the Vlasov equation for the evolution of a phasespace distribution with a small sinusoidal perturbation one can find the threshold and calculate the initial growth rate as a function of $Z_{||}/n$. [17] However, if one needs to know the effect of the instability on a real process in which the instability develops beyond a small perturbation and where, like as not, parameters are changing on a time scale comparable to or faster than the growth time, there are no simple formulas. One can simulate the entire course of the process realistically, but the amount of computing time required may be a practical limitation.

Binning, Statistics, and All That

The particular harmonics of the beam circulation frequency present in the beam current spectrum depend on how the buckets are filled. However, for a typical cutoff frequency of 1.7 GHz the decay time of the wakefield in the $Q = 1$ resonator is $\tau_D = 2Q/\omega \approx 0.2$ ns.

Because this is usually much less than the bunch length it is only necessary to calculate for a single bunch, and it can't make any difference how the ring is filled. The power in the high frequency spectrum will depend on the bunch shape; with the resonance covering many circulation harmonics it matters little exactly how the power is divided between them. These facts make it plausible that one can model the microwave instability problem realistically without including all circulation harmonics. If one takes all harmonics of the rf frequency one can represent the physical situation adequately.[18]

To calculate n amplitudes and phases of the fourier decomposition of the beam current corresponding to a bunch, the azimuthal interval $2\pi/h$ is divided into $2n$ bins. The calculation of the highest frequency component involves an integral like $\int I(\vartheta) \sin n\vartheta d\vartheta$ so that it is roughly a sum of differences of adjacent bin populations. A statistical argument for the number of macroparticles required for the tracking follows from the proposition that the error of the bin populations should be less than the systematic difference between bins. When a smooth distribution is binned into N_B samples, the difference between adjacent bins will be $\sim \mathcal{O}(N_B^{-1})$. The error for the i -th bin is $\mathcal{O}(n_i^{-1/2})$, where n_i is the bin population. The bin population is $\mathcal{O}(N_p/N_B)$, where N_p is the number of macroparticles. Requiring the systematic difference to be greater than the bin error gives

$$\frac{1}{N_B} > \left(\frac{N_B}{N_p} \right)^{\frac{1}{2}} \Rightarrow N_p > N_B^3 . \quad (17)$$

So, for example, for 32 harmonics one needs 2^6 bins and should track $\sim 2^{18} \approx 2.6 \cdot 10^4$ macroparticles. These are numbers which are appropriate to the Main Injector coalescing example treated above. Because the tracking takes $> 10^{-5}$ s/particle-turn even on a fast computer and the debunching requires tens of thousands of turns, the simulation requires hours of computer time.

Coalescing for $I_{\text{beam}} \neq 0$

The part of the bunch coalescing sequence which is critically dependent on the beam intensity and the longitudinal coupling impedance is the debunching of the high frequency bunches to low momentum spread. If the debunching proceeds to the threshold momentum spread and is carried out slowly so that the single particle motion is practically adiabatic, the minimum momentum spread attainable will be about the threshold momentum spread for the instability. To optimize coalescing when beam current is a limiting factor one will explore faster debunching and alternative schemes where the momentum compression is obtained by bunch rotation.

For comparison with the previous result calculated without regard to the effect of the beam current, Main Injector coalescing is modeled with the design parameters of $3 \cdot 10^{11}$ protons for the coalesced bunch and a broadband $Z_{||}/n = 5\Omega$. Figure 6 shows the debunched distribution when the effect of the proton charge is added to the sequence previously shown; it is to be compared with fig. 3. Figure 7 shows how well this can be captured in an $h=588$ bucket after rotation. Other parameters need to be changed to fully optimize the coalescing, but the given result is already better than what is now possible in the Fermilab Main Ring.

Detailed optimization for this example is tedious because the computing time is large. A debunching scheme based on bunch rotation proceeds much faster and is therefore simpler to explore with a modeling approach. However, at this intensity, the voltage reduction debunching is better for the coupling impedance specified.

Remarks

The underlying intention in the foregoing is to introduce basic tools for realistic modeling of the longitudinal phase-space behavior of beams in synchrotrons and storage rings in some detail. The process of coalescing several bunches into one was chosen more to illustrate some of the versatility of these tools than to exhibit a polished optimization. In the ten years or so that ESME has been available, it has been used for everything from quick trials of half-baked ideas to detailed simulation of the dynamics of complex extended processes. In the natural course of things, the first type of application may evolve by degrees into the second when the idea proves promising. Therefore, it is advantageous to employ these tools within an open-ended program design. Although a code can pick up a wide variety of features during years of development, the user should need to be aware only of those relevant to his immediate problem, and he should be able to introduce new features without overall reformulation. ESME has a combination of data-driven program flow and global storage for physically significant variables that has proven rather adaptable and extensible. The tools themselves should be minimally dependent on special features of the higher level code so that they can be easily deployed in more particular programs. In this context the "tools" are the basic equations, not ESME subroutines which embody them, because ESME achieves its flexibility partly through the superstructure of global variables which subroutines can exploit as needed. There is no software toolbox which contains separable modules for generation of distributions, mapping, calculation of beam current effects, plotting, *etc.* Perhaps the next person to write a general program in this area can make a start by designing it with a criterion for full independence of functions to the lowest practical level.

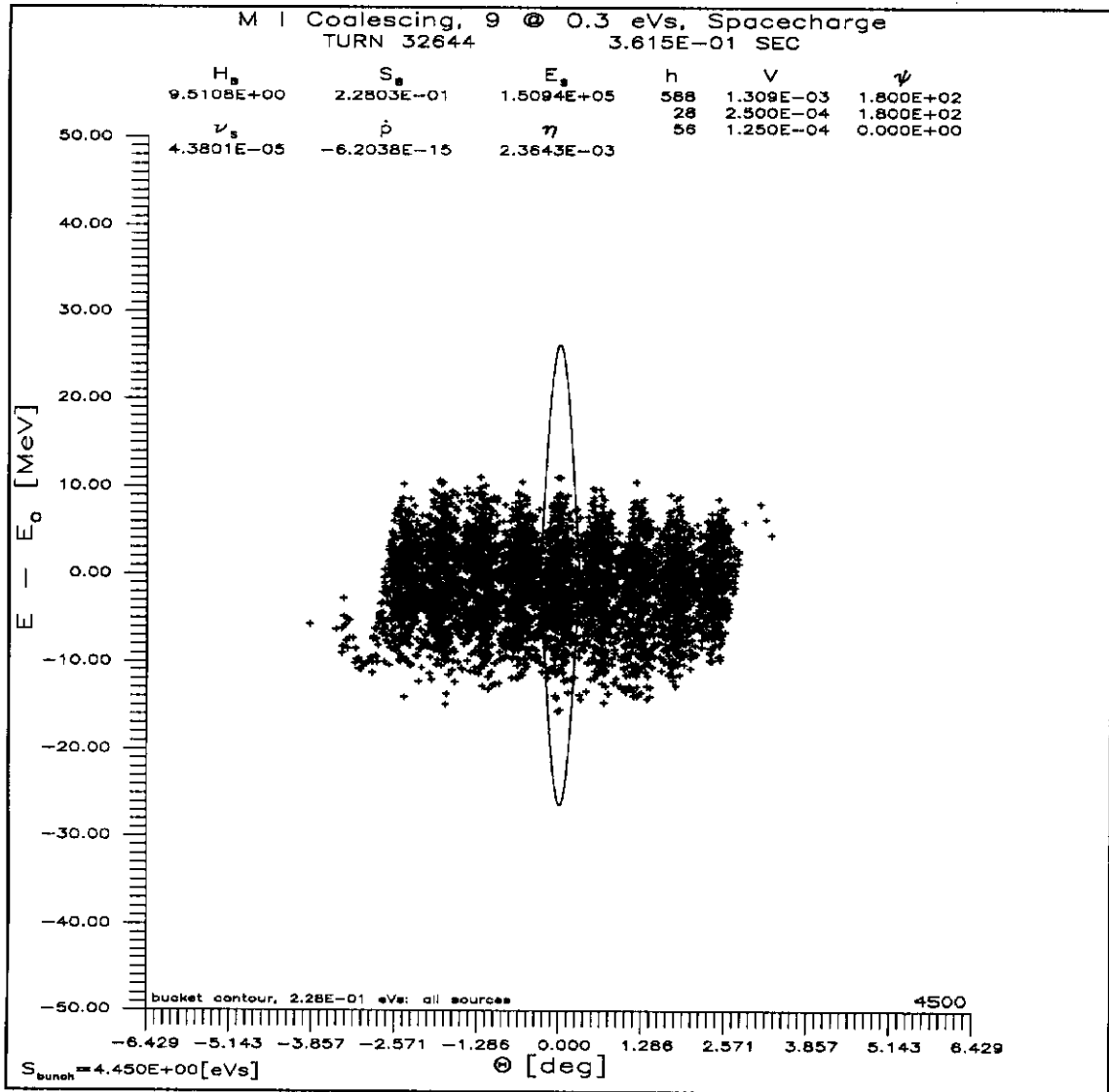


Figure 6: The debunching process at 0.36 s with beam current effects calculated for $3 \cdot 10^{11}$ protons. The distribution may be compared with the zero-current distribution in fig. 3. The high frequency bucket drawn is that corresponding to the initial 10 kV.

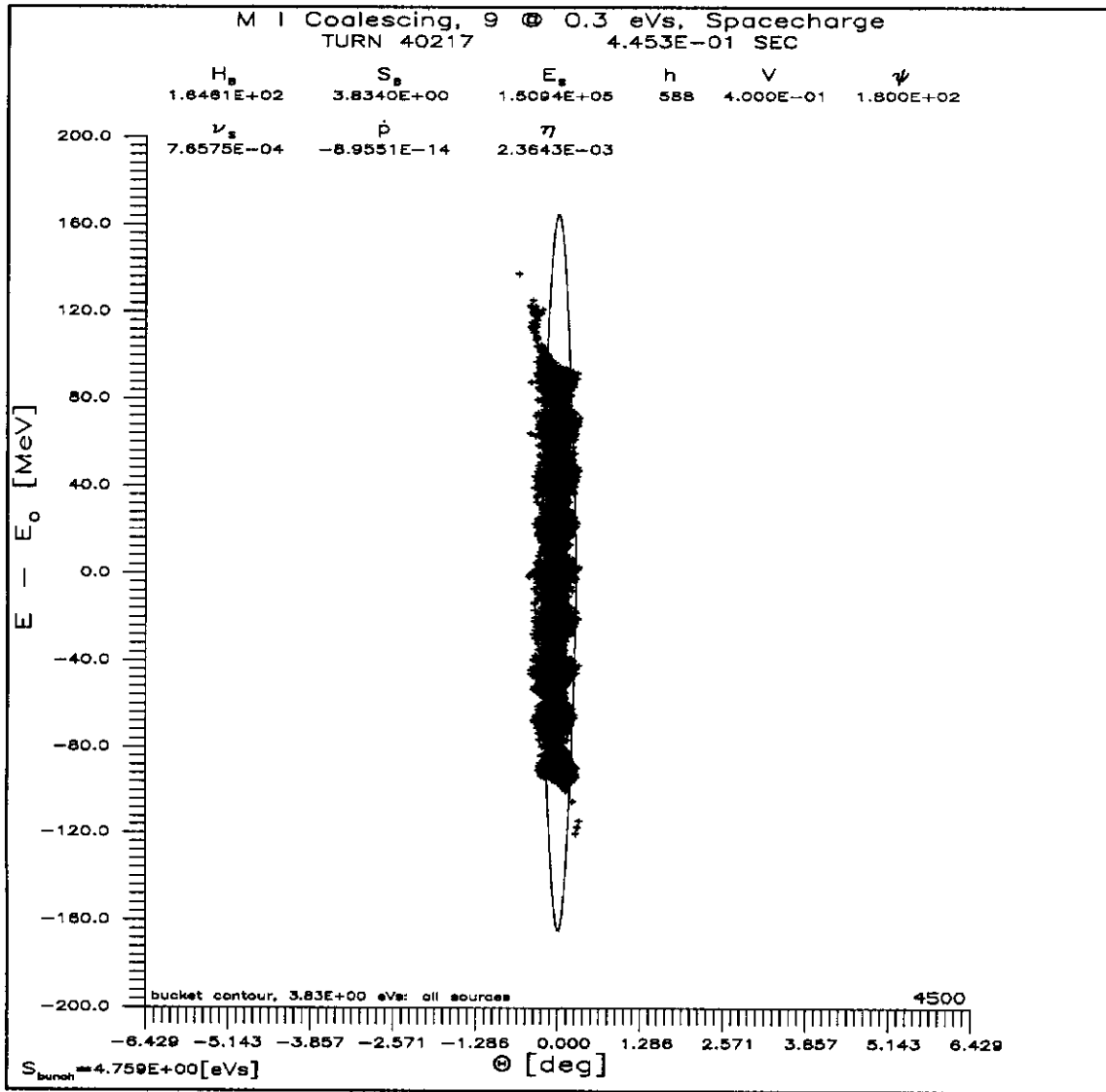


Figure 7: The distribution shown in fig. 6 after rotation in a linearized $h=28$ bucket. The $h=588$ contour indicates the reduced efficiency of the recapture compared with fig. 5.

References

- [1] J. Griffin, J. MacLachlan, A. Ruggiero, and K. Takayama, "Time and Momentum Exchange for Production and Collection of Intense Antiproton Beams at Fermilab", IEEE Trans. on Nucl. Sci. **NS-30** #4, 2360 (Aug. 83)
- [2] J. Griffin, J. MacLachlan, and Z. Qian, "RF Exercises Associated with Acceleration of Intense Antiproton Bunches at Fermilab", IEEE Trans. on Nucl. Sci. **NS-30** #4, 2627 (Aug. 83)
- [3] S. Stahl and J. MacLachlan, "Users Guide to ESME v. 7.1", Fermilab internal note TM-1650 (2/90) and
J. MacLachlan, "An ESME Update (v. 7.2)", Fermilab internal note TM-1716 (11 Feb. 91)
- [4] S. R. Koscielniak, "The LONG1D Simulation Code", Proc. of the European Part. Acc. Conf., v. 1, 743 (1988)
- [5] J. Wei, "Longitudinal Dynamics of the Non-Adiabatic Regime on Alternating Gradient Synchrotrons", Ph.D thesis, SUNY Stonybrook (1990)
- [6] J. MacLachlan, "Difference Equations for Longitudinal Motion in a Synchrotron", Fermilab note FN-529 (15 Dec. 89)
- [7] J. MacLachlan, "Differential Equations for Longitudinal Motion in a Synchrotron", Fermilab note FN-532 (25 Jan. 90)
- [8] P. Lucas and J. MacLachlan, "Transition Jump for the Fermilab Booster", Proc. 1987 IEEE Part. Acc. Conf., 1114 (March 1987)
- [9] A. Hofmann and F. Pedersen, "Bunches with Local Elliptic Energy Distributions", IEEE Trans. on Nucl. Sci. **NS-26** #3, 3526 (3 June 1979)
- [10] J. MacLachlan and J. Griffin, "Debunching Into a Bucket of Lower Harmonic Number", Fermilab internal note TM-1504 (9 December 1987)
- [11] R. Garoby, "Simulation of Bunches Coalescing in the Main Ring in the Presence of a High-Frequency, Wide-Band Resonator", Fermilab internal notes TM-1495 (4 December 1986) and TM-1495-rev (4 December 1986)
- [12] P. Martin, remarks at Fermilab III Instabilities Workshop (June 1990), unpublished
- [13] J. Griffin, "Bunch Coalescing", in Proc. of the Fermilab Instabilities Workshop, Fermilab internal note TM-1696 (June 1990) p91
- [14] J. MacLachlan, "Fundamentals of Particle Tracking for the Longitudinal Projection of Beam Phasespace in Synchrotrons", Fermilab note FN-481 (15 April 88)

- [15] V. K. Neil and A. M. Sessler, "Longitudinal Resistive Instabilities of Intense Coasting Beams in Particle Accelerators", NIM **36** #4, 429 (April 1965)
- [16] J. MacLachlan, "Longitudinal Phasespace Tracking with Space Charge and Wall Coupling Impedance", Fermilab note FN-446 (February 1987)
- [17] A. Hofmann, "Longitudinal Instabilities" in "Theoretical Aspects of the Behavior of Beams in Accelerators and Storage Rings", CERN 77-13 (19 July 1977), p139 ff
- [18] J. MacLachlan, "Limits to Coalescing and Bunch Rotation for \bar{p} Production Resulting from Microwave Instability", in Proc. of the Fermilab III Instabilities Workshop, Fermilab internal note TM-1696 (June 1990) p70